



## Synergistic effect in treatment of C.I. Acid Red 2 by electrocoagulation and electrooxidation

X.D. Zhang<sup>a</sup>, J.D. Hao<sup>a</sup>, W.S. Li<sup>a,b,\*</sup>, H.J. Jin<sup>a</sup>, J. Yang<sup>a</sup>, Q.M. Huang<sup>a,b</sup>, D.S. Lu<sup>a,b</sup>, H.K. Xu<sup>c</sup>

<sup>a</sup> School of Chemistry and Environment, South China Normal University, Guangzhou 510006, China

<sup>b</sup> Key Lab of Electrochemical Technology on Energy Storage and Power Generation in Guangdong Universities, Guangzhou 510631, China

<sup>c</sup> Dongguan Hongjie Environmental Technologies Ltd, Guangdong 523039, China

### ARTICLE INFO

#### Article history:

Received 26 October 2008

Received in revised form 11 May 2009

Accepted 11 May 2009

Available online 19 May 2009

#### Keywords:

Synergistic effect  
Decolorization  
Electrocoagulation  
Electrooxidation  
C.I. Acid Red 2

### ABSTRACT

An aqueous C.I. Acid Red 2 solution was decolorized by electrolysis using iron as anode. The decolorization mechanism was investigated through experimental observations on the electrochemical behavior of C.I. Acid Red 2 on Pt rotating disk electrode, UV–visible spectra of the solution and IR spectra of the coagulated mixtures. It is found that the decolorization efficiency is high, over 98.0% after 40 min, and this high decolorization efficiency can be ascribed to the synergistic effect of electrocoagulation and electrooxidation. The electrocoagulation results from the electrogenerated iron hydroxide and the electrooxidation results from electrogenerated ferric ions. The results obtained from IR spectra shows that the decolorization of C.I. Acid Red 2 by electrooxidation is due to the partial or complete cleavage of C–N bonds in C.I. Acid Red 2.

© 2009 Elsevier B.V. All rights reserved.

### 1. Introduction

Compared with other methods for wastewater treatment, electrochemical technologies have many advantages, convenient, highly efficient and environmentally friendly [1–3], because it does not add extra chemical into the system [4,5]. Added chemical substances might cause the secondary water pollution [6]. Electrocoagulation (EC) as one of the electrochemical technologies has attracted great attention in the wastewater treatment, since it combines oxidation and reduction (indirect or direct), flotation, concentration and collection of the metal hydroxide flocs and adsorbed pollutants by hydrogen gas bubbles formed at the cathode [7–9]. The EC process takes advantage of the binding effect of charge neutralization/surface complexation/adsorption onto the in-situ formed metal hydroxides generated from the oxidation of sacrificial anode materials (e.g. Fe and Al). EC has been used for the treatment of various effluents generated from restaurant [10,11], silicon wafer polishing processes [12] and textile [7,13–17]. It was believed that the removal efficiency of pollutants by the electrochemical coagulation was higher than those by the chemical coagulation [18].

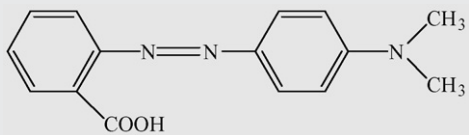
Dye wastewater is an environmental concern due to its huge quantity, variable nature, biologically-difficult-to-degrade chemical composition, and toxicity to aquatic life [19]. EC technology was

widely used for the treatment of dye wastewater. Cañizares et al. [20] reported that the dye molecules were removed by the binding of Eriochrome Black T (EBT) molecules to the surface of small iron or aluminum precipitated particles. Golder et al. [21] studied the decolorization of aqueous solutions of methylene blue (MB) and eosin yellowish (EY) using mild steel electrodes and believed that the decolorization resulted from electrocoagulation. Merzouk et al. [22] used aluminum electrodes as anode electrode to treat a synthetic textile wastewater. The decolorization efficiency and the COD abatement were higher than 80%. Raju et al. [23] reported that the wastewater from a textile industry was initially treated by electrocoagulation and then by electrooxidation. The level of COD of the effluent was high. Szpyrkowicz et al. [24] used electrooxidation technique to treat synthetic textile wastewater containing partially soluble disperse dyes and obtained 39% removal of COD after 40 min of electrolysis and 90% removal of color.

C.I. Acid Red 2 (methyl red) is a representative of organic compounds known as azo-dyes, which is widely used in the textile industries and analytical chemistry. The chemical structure and other characteristics of this dye are shown in Table 1. C.I. Acid Red 2 is resistant to the degradation by light, oxygen and common acids and bases [25]. In this paper, an aqueous C.I. Acid Red 2 solution was treated by electrolysis using carbon steel as anode, with an aim at understanding the mechanism on the decolorization of C.I. Acid Red 2. It was found that there was a synergetic effect of electrooxidation and electrocoagulation in the decolorization of C.I. Acid Red 2, resulting in a high decolorization efficiency.

\* Corresponding author. Tel.: +86 020 39310256; fax: +86 020 39310256.  
E-mail address: [liwsh@scnu.edu.cn](mailto:liwsh@scnu.edu.cn) (W.S. Li).

**Table 1**  
Structure and characteristics of C.I. Acid Red 2.

Dye	C.I. Acid Red 2 (methyl red)
Structure	
$\lambda_{\max}$ (nm)	523
Chemical class	Monoazo
C.I. number	13020
$M$ (g/mol)	269.30

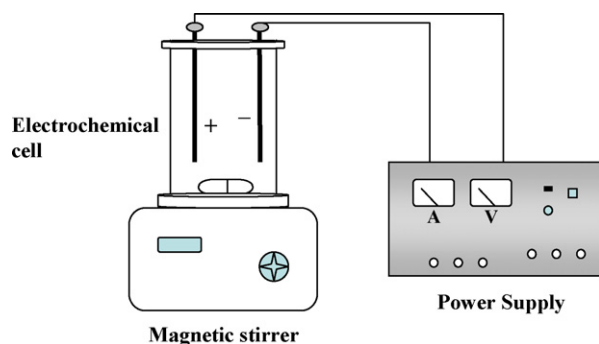


Fig. 1. Schematic diagram of experimental setup.

## 2. Experimental

### 2.1. Electrolysis

Electrolysis experiments were carried out in a batch electrolytic cell, as shown in Fig. 1. Carbon steel was used as anode and stainless steel (grade 316) was used as cathode. The distance between two electrodes during electrolysis was 1 cm and the effective area of the electrodes was 129.2 cm<sup>2</sup>. Before experiment, the electrodes were immersed in 1.0 M HCl solution for 5 min and then rinsed by water. The electrolysis was carried out on a DC power supply under constant current density in the solution containing 100 mg L<sup>-1</sup> C.I. Acid Red 2 and 0.005 mol L<sup>-1</sup> Na<sub>2</sub>SO<sub>4</sub>, pH 3.10, at room temperature and under stirring. Na<sub>2</sub>SO<sub>4</sub>, instead of NaCl which has higher pollutant abatement efficiency, was used as electrolyte because it does not generate adsorbable organically bound halogens (AOX) that can be formed in chloride containing solution [26]. The current density was 2.2 mA/cm<sup>2</sup>. The electrode distance, the concentrations of C.I. Acid Red 2 and Na<sub>2</sub>SO<sub>4</sub>, the pH of the solution, and the current density were selected based on the highest decolorization efficiency. More detailed information on the relation of the decolorization efficiency with electrolysis conditions will be reported in another paper.

### 2.2. Sweeping voltammetry

Sweeping voltammetric measurements were performed on a Pt rotating disc ( $d = 3$  mm) by an Autolab PGSTAT-30 (Eco Echemine BV Inc.), in 0.1 mol L<sup>-1</sup> Na<sub>2</sub>SO<sub>4</sub> solution with and without 100 mg L<sup>-1</sup> C.I. Acid Red 2 at room temperature. A platinum wire was used as the counter electrode and an Ag/AgCl electrode as a reference electrode. The potentials in this paper were with respect to this reference. Before sweeping voltammetric measurements, the working electrode was polished with 0.05  $\mu$ m alumina, cleaned by ultrasonication in acetone and distilled water successively, and then cycling in 0.5 M H<sub>2</sub>SO<sub>4</sub> between 0.2 and 0.9 V at 100 mV s<sup>-1</sup>.

### 2.3. Chemical and spectroscopic analyses

For the decolorization efficiency analyses, the solution was filtered through 0.45  $\mu$ m millipore membrane filter to remove iron hydroxide flocs. The concentration of C.I. Acid Red 2 was determined from the UV absorbance recorded at 523 nm ( $\lambda_{\max}$ ) by a Shimadzu model UV-1700 double-beam spectrophotometer and the decolorization efficiency (%DE) was calculated from [27]:

$$\%DE = \frac{A_0 - A_t}{A_0} \times 100\% \quad (1)$$

where,  $A_0$  and  $A_t$  are the absorbance of the solution initially and at time  $t$ , respectively. The molar extinction coefficient of Acid Red 2 in the acidic (working) pH range at 523 nm was  $1.48 \times 10^3$  L mol<sup>-1</sup> cm<sup>-1</sup>.

The chemical oxygen demand (COD) in the solution was determined by the standard method involving potassium dichromate. The COD reduction rate of the solution was obtained by the following equation:

$$\%COD \text{ reduction} = \frac{[(COD)_0 - (COD)_t]}{(COD)_0} \times 100\% \quad (2)$$

where  $(COD)_0$  and  $(COD)_t$  are the chemical oxygen demand of the solution before treatment and after treatment for a certain time, respectively.

Fourier Transform Infrared Spectroscopy (FT-IR) was recorded from 4000 to 450 cm<sup>-1</sup> on Perkin Elmer instruments (Spectrum One FT-IR Spectrometer). The coagulated mixture was isolated from the tank and then dried at 40 °C (vacuum) to a constant weight. At last, the coagulated mixture was mixed with KBr and pressed into a disk for FT-IR analysis.

## 3. Results and discussion

### 3.1. Decolorization efficiency

The decolorization efficiency as a function of treatment time was obtained with a constant current of 2.2 mA/cm<sup>2</sup>, in the solution containing 100 mg/dm<sup>3</sup> C.I. Acid Red 2 and 0.005 M Na<sub>2</sub>SO<sub>4</sub>, pH 3.10. The result is shown in Fig. 2. It can be seen from Fig. 2 that the decolorization efficiency drastically increases in the first 20 min, reaching over 80%. In the later 20 min, the decolorization efficiency increases slightly but reaches 98.0% after 40 min. The decolorization of C.I. Acid Red 2 should be related to the electrocoagulation because the mild steel is used as the anode. In fact, the coagulated mixture

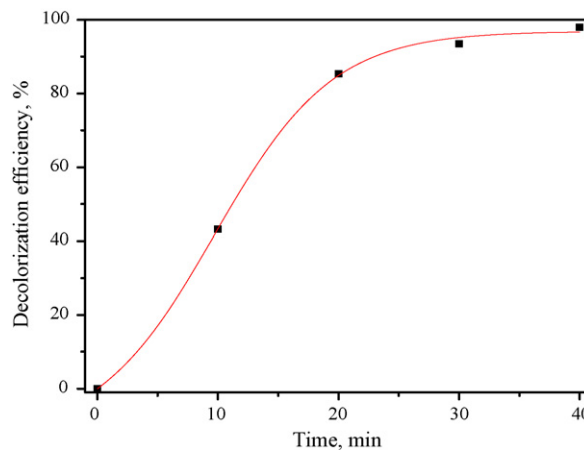


Fig. 2. The decolorization efficiency as a function of treatment time. Conditions: 0.005 M Na<sub>2</sub>SO<sub>4</sub>, initial pH 3.10, initial C.I. Acid Red 2 100 mg/dm<sup>3</sup>, applied current density 2.2 mA/cm<sup>2</sup>.



**Fig. 3.** Schematic diagram of the coagulated mixtures distribution in the electrochemical cell.

can be observed above the solution after electrolysis. It consists of two layers, the first layer is red and the second layer is black green, as shown in Fig. 3.

However, the decolorization efficiency in this work is higher than the results reported in literatures on the treatment of C.I. Acid Red 2 containing solutions. For example, Zhou et al. [28] studied the treatment of C.I. Acid Red 2 solution using electro-Fenton technology and obtained the highest decolorization efficiency of the solution was about 80%. Thus besides the electrocoagulation, there might be other factors that favors the removal of C.I. Acid Red 2. To understand the mechanism on the decolorization of C.I. Acid Red 2, the anodic oxidation behavior of C.I. Acid Red 2 and the composition of the coagulated mixtures formed in solution during electrolysis were investigated.

### 3.2. Anodic oxidation of C.I. Acid Red 2

Fig. 4 presents the cyclic voltammograms of Pt rotating disk electrode in 0.1 M  $\text{Na}_2\text{SO}_4$  solutions with and without C.I. Acid Red 2. Comparing the voltammogram of the solution containing C.I. Acid Red 2 (curve b of Fig. 4) with that of the C.I. Acid Red 2 free solution (curve a of Fig. 4), it can be seen that the oxidation currents in the solution containing C.I. Acid Red 2 are larger in the potential range between 0.8 V and 1.3 V, and the currents (oxidation or reduction) in the other potential range are equal or smaller than those in the solution without C.I. Acid Red 2. This indicates that C.I. Acid Red 2 can be oxidized, but not reduced. Thus the removal of the C.I. Acid Red 2 might be related to its oxidation.

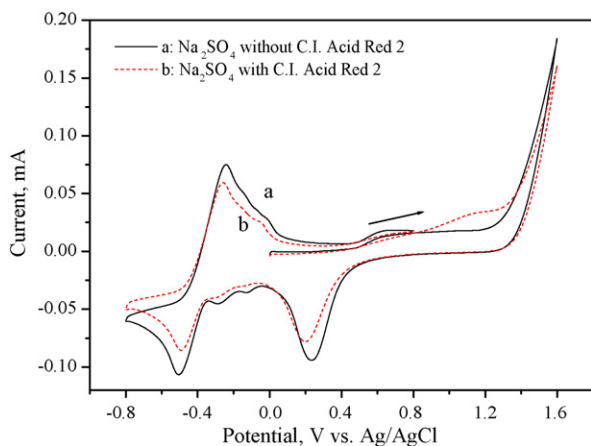


**Fig. 4.** The Cyclic voltammograms on Pt rotating disk electrode: (a) supporting electrolyte; (b) supporting electrolyte containing C.I. Acid Red 2, pH 3.1. Scan rate: 0.1 V/s, rotating rate: 600 rpm.

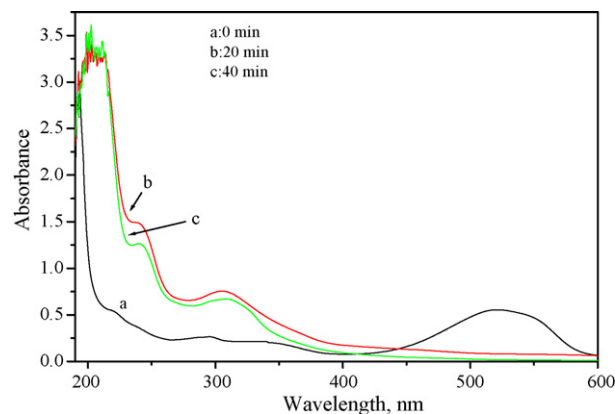


**Fig. 5.** The absorbance spectra of dye solutions containing C.I. Acid Red 2 before and after electrolysis experiments. Conditions: 0.005 M  $\text{Na}_2\text{SO}_4$ , initial pH 3.10, initial C.I. Acid Red 2 100 mg/dm<sup>3</sup>, applied current density 2.2 mA/cm<sup>2</sup>.

### 3.3. UV-visible spectra

Fig. 5 presents the UV-visible absorbance spectra of the solution containing 100 mg/dm<sup>3</sup> C.I. Acid Red 2 at different time during electrolysis. C.I. Acid Red 2 is characterized by two absorbance peaks of 290 nm and 215 nm in ultraviolet region and one peak of 523 nm in visible region, as shown by the curve a of Fig. 5. The absorbance in visible region should be ascribed to the chromophore group of  $-\text{N}=\text{N}-$  and the absorbance in ultraviolet region should be ascribed to the benzene ring and the carbonyl group. After electrolysis, the absorbance of the solution in the visible region disappears, as shown by the curves b and c of Fig. 5. On the other hand, the absorbance of the solution in ultraviolet region is stronger after electrolysis and becomes weaker as electrolysis proceeds. This suggests that the decolorization of the solution involves the decomposition of C.I. Acid Red 2 through the breaking of  $-\text{N}=\text{N}-$ . Based on the result obtained from sweeping voltammetry, the decomposition is an oxidation reaction.

### 3.4. IR spectra

Fig. 6 presents IR spectra of the coagulated mixtures. The mixtures were sampled from the two layers of Fig. 3 separately and dried at 40 °C (vacuum) to a constant weight before IR analysis. The curve a of Fig. 6 is the IR spectra of C.I. Acid Red 2. The curves b and c of Fig. 6 show the IR spectra of the coagulated mixture in first layer and second layer, respectively. As seen in the curve a of Fig. 6, the absorbance peaks at 1502 cm<sup>-1</sup>, 1473 cm<sup>-1</sup>, 1227 cm<sup>-1</sup>,

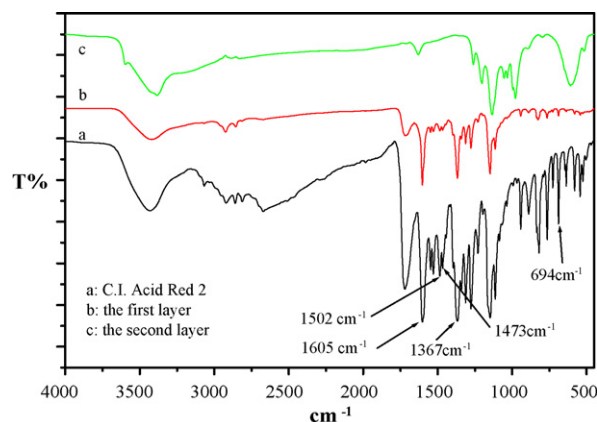
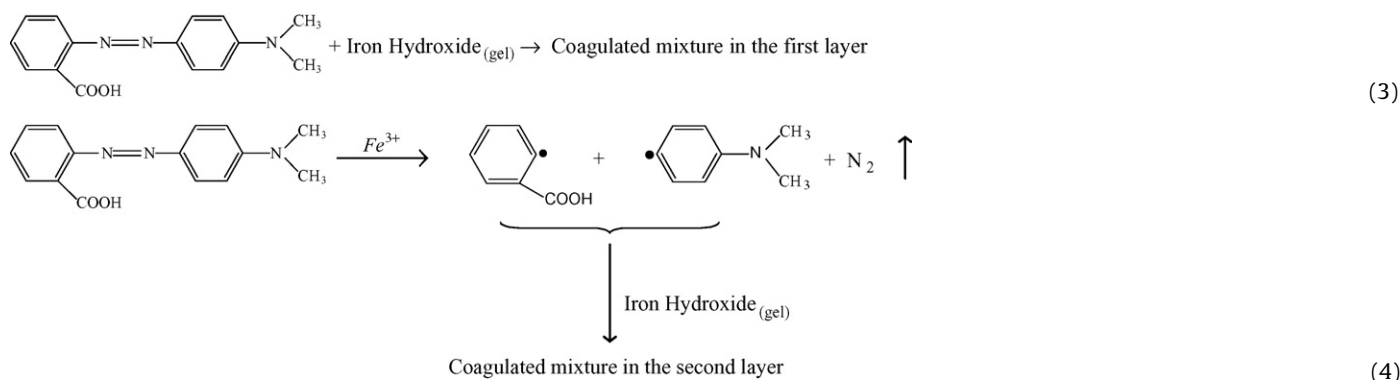


**Fig. 6.** FT-IR spectra of the samples of (a) C.I. Acid Red 2; (b) the first layer; (c) the second layer.

and  $694\text{ cm}^{-1}$  are corresponding to the group  $-\text{N}=\text{N}-$  [29], and the absorbance peaks  $1367\text{ cm}^{-1}$  and  $1605\text{ cm}^{-1}$  are corresponding to the groups  $\text{C}-\text{N}$  of the  $\text{C}-\text{N}=\text{N}-\text{C}$  [25] and benzene ring, respectively. This indicates that the coagulated mixture in the first layer contains the primary dye molecule, C.I. Acid Red 2. That is to say, C.I. Acid Red 2 is coagulated by the iron hydroxide at the beginning of the electrolysis. However, the coagulated mixture in the second layer shows very different IR spectrum in which the peaks corresponding to groups  $-\text{N}=\text{N}-$  and  $\text{C}-\text{N}$  disappear and the peak corresponding to the benzene ring remains, as shown by the curve c of Fig. 6. This is suggested that in the later period of the electrolysis, C.I. Acid Red 2 experiences a reaction through the breaking of the bond  $\text{C}-\text{N}$ , forming benzene-containing molecules which are coagulated by the iron oxide.

With the results available, the mechanism on the decolorization of C.I. Acid Red 2 solution can be inferred as follows:



C.I. Acid Red 2 is first coagulated by the iron hydroxide at the beginning of the electrolysis, forming the first layer of the coagulated mixture shown in Fig. 3. This layer looks red because the mixture mainly consists of C. I. Acid Red 2 and ferric hydroxide. C.I. Acid Red 2 may be oxidized by ferric ions in the solution or directly on the anode through the breaking of the bond  $\text{C}-\text{N}$  of the  $\text{C}-\text{N}=\text{N}-\text{C}$  group in the later period of the electrolysis, forming benzene-containing molecules. However, as Fig. 4 shows, the oxidation of C.I. Acid Red 2 takes place at  $0.8\text{ V}$  vs.  $\text{Ag}/\text{AgCl}$  on Pt electrode. Carbon steel employed as anode had been dissolved at this potential. Therefore, only the indirect oxidation by ferric ions but not the direct oxidation of C.I. Acid Red 2 on anode contributes to the breaking of the bond  $\text{C}-\text{N}$  group. The benzene-containing molecules from the breaking of the  $\text{C}-\text{N}$  group are also coagulated by the iron hydroxide, forming the second layer of the coagulated

mixture shown in Fig. 3. This second layer looks black green because it contains colorless benzene-containing molecules, ferric hydroxide and ferrous hydroxide formed from the reduction of ferric ions. Inevitably, the benzene-containing molecules from the breaking of the  $\text{C}-\text{N}$  group also exist in the first layer of the coagulated mixture.

### 3.5. COD reduction rate

The chemical oxygen demand (COD) of the solution was evaluated by the standard method involving potassium dichromate. Fig. 7 shows the variation of the COD reduction rate in the solution with the electrolysis time. It can be seen from Fig. 7 that the variation of the COD reduction rate is similar to that of decolorization efficiency (Fig. 2). However, the COD reduction rate after the electrolysis is low,

only 33% at 40 min compared the high decolorization efficiency, 98.0%. This suggests that the products from the oxidation of C. I. Acid Red 2 cannot be removed completely. This was confirmed by potential measurement. The potential of platinum in the solution before and after treatment is  $0.43\text{ V}$  and  $0.44\text{ V}$ , respectively. Therefore, further treatment should be considered in order to improve the COD reduction rate of the solution containing C. I. Acid Red 2.

## 4. Conclusions

The solution containing C.I. Acid Red 2 (methyl red) can be decolorized by electrolysis using carbon steel as the anode. A high decolorization efficiency, 98.0%, can be achieved. This high decolorization efficiency results from the synergistic effect of electrocoagulation and electrooxidation. At the beginning of the electrolysis, C.I. Acid Red 2 is coagulated by ferric hydroxide. At the latter of the electrolysis, C.I. Acid Red 2 is oxidized by ferric ions in the solution, forming colorless benzene-containing molecules which is also coagulated by ferric hydroxide.

## References

- [1] O.T. Can, M. Bayramoglu, M. Kobya, Decolorization of reactive dye solutions by electrocoagulation using aluminum electrodes, *Ind. Eng. Chem. Res.* 42 (2003) 3391–3396.
- [2] M.H. Zhou, Q.Z. Dai, L.C. Lei, C. Ma, D. Wang, Long life modified lead dioxide anode for organic waste water treatment: electrochemical characteristics and degradation mechanism, *Environ. Sci. Technol.* 39 (2005) 363–370.
- [3] X.D. Zhang, W.S. Li, Y.J. Huang, H.Y. Peng, Promotion of oxygen reduction reaction on vitreous carbon electrode by DTAB, *Acta Phys. – Chim. Sinica* 24 (4) (2008) 691–694.
- [4] S. Chou, Y.H. Huang, S.N. Lee, G.H. Huang, C. Huang, Treatment of high strength hexamine-containing wastewater by Electro-Fenton method, *Water Res.* 33 (3) (1999) 751–759.
- [5] S.H. Lin, C.C. Chang, Treatment of landfill leachate by combined electro-fenton oxidation and sequencing batch reactor method, *Water Res.* 34 (17) (2000) 4243–4249.
- [6] N. Azbar, T. Yonar, K. Kestioglu, Comparison of various advanced oxidation processes and chemical treatment methods for COD and color removal from

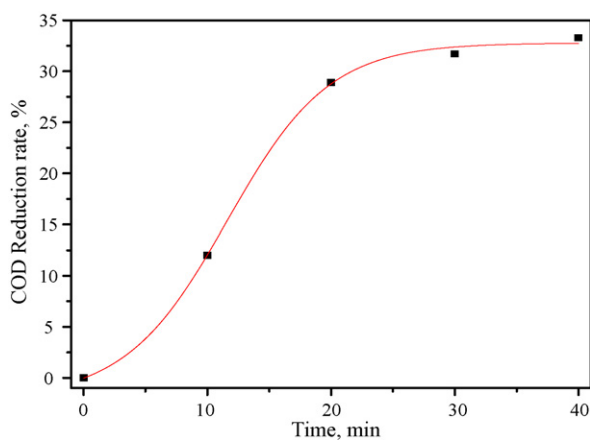


Fig. 7. The variation of COD reduction rate of the solution during electrolysis. Conditions:  $0.005\text{ M Na}_2\text{SO}_4$ , initial pH 3.10, initial C.I. Acid Red 2  $100\text{ mg}/\text{dm}^3$ , applied current density  $2.2\text{ mA}/\text{cm}^2$ .

- a polyester and acetate fiber dyeing effluent, *Chemosphere* 55 (2004) 35–43.
- [7] X.M. Chen, G.H. Chen, F.R. Gao, P.L. Yue, High-performance Ti/BDD electrodes for pollutant oxidation, *Environ. Sci. Technol.* 37 (2003) 5021–5026.
- [8] K. Rajeshwar, J.G. Ibanez, G.M. Swai, *Electrochemistry and the environment*, J. Appl. Electrochem. 24 (1994) 1077–1091.
- [9] A. Reife, H.S. Freeman, *Environmental Chemistry of Dyes and Pigments*, John Wiley & Sons, Inc., Canada, 1996, pp. 329–330.
- [10] M.Y.A. Mollah, P. Morkovsky, J.A.G. Gomes, M. Kesmez, J. Parga, D.L. Cocke, Fundamentals, present and future perspectives of electrocoagulation, *J. Hazard. Mater.* B114 (2004) 199–210.
- [11] X.M. Chen, G.H. Chen, P.L. Yue, Separation of pollutants from restaurant wastewater by electrocoagulation, *Sep. Purif. Technol.* 19 (1–2) (2000) 65–76.
- [12] W. Den, C.P. Huang, H.C. Ke, Mechanistic study on the continuous flow electrocoagulation of silica nanoparticles from polishing wastewater, *Ind. Eng. Chem. Res.* 45 (2006) 3644–3651.
- [13] Y. Xiong, P.J. Strunk, H. Xia, X. Zhu, H.T. Karlsson, Treatment of dye wastewater containing acid orange II using a cell with three-phase three-dimensional electrode, *Water Res.* 35 (2001) 4226–4230.
- [14] I. Arslan-Alaton, I. Kabdasli, D. Hanbaba, E. Kuybu, Electrocoagulation of a real reactive dyebath effluent using aluminum and stainless steel electrodes, *J. Hazard. Mater.* 150 (1) (2008) 166–173.
- [15] A. Alinsafi, M. Khemis, M.N. Pons, J.P. Leclerc, A. Yaacoubi, A. Benhammou, A. Nejmeddine, Electro-coagulation of reactive textile dyes and textile wastewater, *Chem. Eng. Process.* 44 (2005) 461–470.
- [16] A. Gurses, M. Yalcin, C. Dogar, Electrocoagulation of some reactive dyes: a statistical investigation of some electrochemical variables, *Waste Manage.* 22 (2002) 491–499.
- [17] S. Song, J. Yao, Z.Q. He, J.P. Qiu, J.M. Chen, Effect of operational parameters on the decolorization of C.I. Reactive Blue 19 in aqueous solution by ozone-enhanced electrocoagulation, *J. Hazard. Mater.* 152 (1) (2008) 204–210.
- [18] A.G. Vlyssides, D. Papaioannou, M. Loizidou, P.K. Karlis, A.A. Zorpas, Testing an electrochemical method for treatment of textile dye wastewater, *Waste Manage.* 20 (2000) 569.
- [19] A. Gürses, M. Yalçin, C. Dögar, Electrocoagulation of some reactive dyes: a statistical investigation of some electrochemical variables, *Waste Manage.* 22 (2002) 491.
- [20] P. Cañizares, F. Martínez, C. Jiménez, J. Lobato, M.A. Rodrigo, Coagulation and electrocoagulation of wastes polluted with dyes, *Environ. Sci. Technol.* 40 (2006) 6418–6424.
- [21] A.K. Golder, N. Hridaya, A.N. Samanta, S. Ray, Electrocoagulation of methylene blue and eosin yellowish using mild steel electrodes, *J. Hazard. Mater.* B127 (2005) 134–140.
- [22] B. Merzouk, B. Gourich, A. Sekki, K. Madani, Ch. Vial, M. Barkaoui, Studies on the decolorization of textile dye wastewater by continuous electrocoagulation process, *Chem. Eng. J.* 149 (1–3) (2009) 207–214.
- [23] G.B. Raju, M.T. Karupiah, S.S. Latha, S. Parvathy, S. Prabhakar, Treatment of wastewater from synthetic textile industry by electrocoagulation–electrooxidation, *Chem. Eng. J.* 144 (1) (2008) 51–58.
- [24] L. Szpyrkowicz, C. Juzzolino, S.N. Kaul, S. Daniele, M.D. De Faveri, Electrochemical oxidation of dyeing baths bearing disperse dyes, *Ind. Eng. Chem. Res.* 39 (9) (2000) 3241–3248.
- [25] S.S. Vaghela, A.D. Jethva, B.B. Mehta, S.P. Dave, S. Adimurthy, G. Ramachandriah, Laboratory studies of electrochemical treatment of industrial azo dye effluent, *Environ. Sci. Technol.* 39 (2005) 2848–2855.
- [26] I. Arslan-Alaton, I. Kabdasli, B. Vardar, O. Tünay, Electrocoagulation of simulated reactive dyebath effluent with aluminum and stainless steel electrodes, *J. Hazard. Mater.* 164 (2009) 1586–1594.
- [27] N. Daneshvar, A.R. Khataee, N. Djafarzadeh, The use of artificial neural networks (ANN) for modeling of decolorization of textile dye solution containing C.I. Basic Yellow 28 by electrocoagulation process, *J. Hazard. Mater.* 137 (2006) 1788–1795.
- [28] M.H. Zhou, Q.H. Yu, L.C. Lei, The preparation and characterization of a graphite PTFE cathode system for the decolorization of C.I. Acid Red 2, *Dyes Pigments* 77 (1) (2008) 129–136.
- [29] Z.M. Shen, J. Yang, X.F. Hu, Y.M. Lei, X.L. Ji, J.P. Jin, W.H. Wang, Dual electrodes oxidation of dye wastewater with gas diffusion cathode, *Environ. Sci. Technol.* 39 (2005) 1819–1826.